ISSN 2616-5775 Vol. 9, Issue 8: 98-106, DOI: 10.25236/AJCIS.2026.090812

High precision simulation of ship obstacle avoidance trajectory motion based on improved particle swarm optimization algorithm

Sha Depeng, Chang Yunlong, Xie Jinpeng

Naval Aviation University, Yantai, China
781356539@qq.com

Abstract: *In order to optimize the control direction of ship obstacle avoidance trajectory, improve the stability and safety of ship maneuvering, a high-precision simulation model of ship obstacle avoidance trajectory motion based on improved particle swarm optimization algorithm is proposed. The parameter model and kinematic model of ship obstacle avoidance trajectory motion are constructed, considering various constraint conditions such as obstacle avoidance, energy consumption minimization, and time efficiency optimization. The constraint function of ship obstacle avoidance trajectory motion planning is constructed, and the improved particle swarm optimization algorithm is used to achieve the optimal parameter regression analysis and solution of ship obstacle avoidance. PSO with rotating surface transformation is adopted Algorithm monitors the current optimal function value of each particle, and when it falls into a local minimum, collision avoidance is achieved through the artificial potential field method that jumps out of ship dynamic targets and static obstacles. The target point position factor is introduced to improve the gravitational potential field function, achieving high-precision planning and design of ship obstacle avoidance trajectory motion. The simulation results show that using this method for ship obstacle avoidance trajectory simulation can guide the target to avoid obstacles, with the characteristics of low computational complexity and strong real-time performance, improving the efficiency of data, and increasing the accuracy of ship collision avoidance from 82.5% before improvement to 92.5%.*

Keywords: *improved particle swarm algorithm; Ship obstacle avoidance; tracks; artificial potential field*

1. Introduction

With the rapid development of intelligent and digital technology, the application of unmanned boats and other water vessels is becoming increasingly widespread, including maritime surveillance, maritime search and rescue, reconnaissance and patrol, special operations support, and environmental monitoring [1-2]. As a key tool for expanding into deep sea and ocean, boats are developing towards multifunctionality, automation, intelligence, unmanned and networked directions. Autonomous boats equipped with unmanned systems have become a research and development trend. Innovative technology modules for surface ships and unmanned boats mainly include path planning module, communication module, autonomous decision-making module, object detection and recognition module, etc [3]. As one of the key technologies for surface unmanned vessels, collision avoidance path planning is of great significance not only for autonomous navigation of surface unmanned vessels, but also for improving the maneuverability and safety of ships by studying high-precision simulation models of ship obstacle avoidance trajectory motion.

The core idea of obstacle avoidance path planning for ships is to calculate the collision free path connecting the starting point and destination, and optimize the obtained path in terms of safety, total length, turning angle, and many other factors. Path planning is a key module for unmanned surface vehicles. Path planning is the process of finding the optimal path from the starting point to the endpoint, taking into account various constraints such as obstacle avoidance, minimizing energy consumption, and optimizing time efficiency to ensure that unmanned systems can safely and efficiently complete their assigned tasks. In reference [4], an improved A * algorithm for the heuristic function was proposed, which added partition distance information and angle variable information, which can shorten the navigation distance and improve the phenomenon of line jitter or even jamming. In reference [5], based on Theta *, improvements were made by conducting 3D Euclidean space search in

ISSN 2616-5775 Vol. 9, Issue 8: 98-106, DOI: 10.25236/AJCIS.2026.090812

all directions, which can reduce the impact of yaw and heading angle limitations on ships during real-time maneuvering. In reference [6], a FO A * algorithm based on ship domain theory is proposed, which can optimize the route after the entire path planning is completed. The FO A * algorithm does not restrict the angle and has discontinuous point positions, making it more suitable for ship tracking and navigation. The traditional genetic algorithm simulates the natural evolution process to search for the optimal solution, which has the characteristics of good adaptability, strong robustness, is not easily trapped in local optima, and is conducive to global optimization. However, it is prone to premature convergence and slow convergence speed.

In response to the drawbacks of traditional methods, this paper proposes a high-precision simulation model for ship obstacle avoidance trajectory motion based on improved particle swarm optimization algorithm. Firstly, the parameter model and kinematic model of ship obstacle avoidance trajectory motion are constructed, and the PSO algorithm with rotating surface transformation is used to monitor the current optimal function value of each particle. Then, the target point position factor is introduced to improve the gravitational potential field function, achieving high-precision planning and design of ship obstacle avoidance trajectory motion. Finally, simulation tests were conducted to demonstrate the superior performance of the proposed method in improving the accuracy of ship obstacle avoidance trajectory motion.

2. Ship obstacle avoidance trajectory parameter model and kinematic model

2.1 Model of ship obstacle avoidance trajectory parameters

Considering the maneuverability of small unmanned boats, medium unmanned boats, as well as large and super large unmanned boats, the maneuverability indices K and T were used to calculate the turning time. Therefore, the time lag of the ship's response to the steering angle after steering is smaller, the rudder response is faster, and the boat enters a steady rotation faster, indicating better followability. However, when the T value is negative, it indicates that the boat's heading is unstable. Set the maneuverability constraint coefficient based on the length of the turning time to facilitate the setting of the objective function. The specific formula is:

$$D = (1-\lambda)\frac{\varepsilon_{i,\max} - \varepsilon_{\mathrm{Y}}}{\varepsilon_u - \varepsilon_{\mathrm{Y}}} + \lambda\sum_{i=1}^{N}\frac{\varepsilon_i - \varepsilon_{\mathrm{Y}}}{\varepsilon_u - \varepsilon_{\mathrm{Y}}} \tag{1}$$

In the formula: $\varepsilon_{i,\max}$ is the rudder response time; ε_{Y} is heading; ε_i is the steering angle; Take the strain value corresponding to the ultimate strength point of the hull plate under monotonic loading; λ =0.0081; The maneuverability of watercraft varies significantly depending on its type, structure, and size.

Accurately judging the situation encountered is a prerequisite for avoiding collisions. When making collision avoidance decisions, it is necessary to analyze the encounter situation of the ship based on COLREGs. The encounter situation of the ship can be divided into head-on encounter and starboard crossing encounter, and the encounter formula is obtained as follows:

$$\sigma_{\mathrm{Y},i+1} = (1-\chi_1 D_i)\sigma_{\mathrm{Y},i} \tag{2}$$

$$E_{i+1} = (1-\chi_2 D_i)E_i \tag{3}$$

In the equation, $\sigma_{\mathrm{Y},i}$ and $\sigma_{\mathrm{Y},i+1}$ represent the i-th and i+1th time, respectively, when two ships intersect at a large angle on the starboard side; SD and SD are the heading angles of the target ship for the i-th and i+1 times, respectively.

Changing course is the most effective action to avoid collisions at close range when the energy density factor S reaches the critical value SC, as shown in the following equation:

$$S_C = \frac{K_{IC}^2}{8\pi\mu}(1-k) \tag{4}$$

The spatial collision risk is determined by the nearest encounter distance, the safe encounter

ISSN 2616-5775 Vol. 9, Issue 8: 98-106, DOI: 10.25236/AJCIS.2026.090812

distance d_1 of the ship, and the safe passage distance d_2 of the ship. Based on this, the ship obstacle avoidance trajectory parameter model considers various constraint conditions, such as obstacle avoidance, energy consumption minimization, and optimal time efficiency, and constructs a constraint function for ship obstacle avoidance trajectory operation planning.

2.2. Kinematic parameter model for ship obstacle avoidance

The spatial collision risk is determined by the nearest encounter distance, ship safety encounter distance d_1, and ship safety passage distance d_2. Using a quadruple ship domain model, the expansion angle satisfies the following equation:

$$\theta_c = \arccos\frac{3K_{II}^2 \pm \sqrt{K_I^4 + 8K_I^2K_{II}^2}}{K_I^2 + 9K_{II}^2} \tag{5}$$

For obstacles and dynamic vessels, it should be ensured that they are outside the area, K_{II}=0), The extended angle of vigilance for ships coming from the right side is θ_c=0 °. Do not process the four asymmetric elliptical like regions in the model to calculate the boundary values of the ship domain [7]. The initial deflection is generally simplified using the lowest order (first-order) buckling mode, and assuming that the longitudinal additional deflection in the bow and stern directions only increases the deflection amplitude without changing the deflection shape, then:

$$\begin{cases} w_0 = W_0 \sin\dfrac{m\pi x}{a}\sin\dfrac{\pi y}{b} \\ w = W\sin\dfrac{m\pi x}{a}\sin\dfrac{\pi y}{b} \end{cases} \tag{6}$$

In the formula, W_0 and W respectively represent the lateral radii on the starboard and port sides.

By substituting the gain of the distance and the gain of the rotation diameter, the expression of the stress function F can be solved as follows:

$$F = \frac{E}{32}(W^2 - W_0^2)\left(\frac{a^2}{m^2b^2}\cos\frac{2m\pi x}{a} + \frac{m^2b^2}{a^2}\cos\frac{2\pi y}{b}\right) - \frac{y^2}{2}\sigma \tag{7}$$

When the side angle of the target ship is at the boundary value of the ship domain with different side angles of the target ship, the ship domain (σ_{xp}, σ_{yp} and τ_{xyp}), and the time collision risk are composed of two parts: the most recently encountered time force, namely:

$$\sigma_x = \sigma_{xp} + \sigma_{xb}, \quad \sigma_y = \sigma_{yp} + \sigma_{yb}, \quad \tau = \tau_{xyp} + \tau_{xyb} \tag{8}$$

Considering various constraints such as obstacle avoidance, minimizing energy consumption, and optimizing time efficiency, the following expressions are obtained between the components:

$$\sigma_{xp} = \frac{\partial^2 F}{\partial y^2} \qquad \sigma_{yp} = \frac{\partial^2 F}{\partial x^2} \qquad \tau_{xyp} = -\frac{\partial^2 F}{\partial x \partial y} \tag{9}$$

By substituting the membership function F, the latest avoidance distance for the road and ship can be obtained:

$$\begin{cases} \sigma_{xp} = \dfrac{\partial^2 F}{\partial y^2} = -\dfrac{m^2\pi^2 E(W^2 - W_0^2)}{8a^2}\cos\dfrac{2\pi y}{b} - \sigma \\ \sigma_{yp} = \dfrac{\partial^2 F}{\partial x^2} = -\dfrac{\pi^2 E(W^2 - W_0^2)}{8b^2}\cos\dfrac{2m\pi x}{a} \\ \tau_{xyp} = -\dfrac{\partial^2 F}{\partial x \partial y} = 0 \end{cases} \tag{10}$$

ISSN 2616-5775 Vol. 9, Issue 8: 98-106, DOI: 10.25236/AJCIS.2026.090812

According to the tracking and turning characteristics of the watercraft, maneuverability constraint coefficients were set separately to provide maneuverability constraints for unmanned surface vessels of different ship sizes during the process of setting collision avoidance paths [8]. The component expression is obtained as follows:

$$\begin{cases} \varepsilon_{xp} = \dfrac{1}{E}(\sigma_{xp} - \nu\sigma_{yp}) \\ \varepsilon_{yp} = \dfrac{1}{E}(\sigma_{yp} - \nu\sigma_{xp}) \\ \gamma_{xyp} = \dfrac{2(1+\nu)}{E}\tau_{xyp} = 0 \end{cases} \tag{11}$$

At the same time, based on the collision risk models of spatial collision risk and temporal collision risk, the strain parameters of the tracking search process are obtained, and the expression of the obstacle avoidance strain component caused is as follows

$$\begin{cases} \varepsilon_{xb} = -z\dfrac{\partial^2}{\partial x^2}(w - w_0) = \mathrm{z}\dfrac{m^2\pi^2}{a^2}(W - W_0)\sin\dfrac{m\pi x}{a}\sin\dfrac{\pi y}{b} \\ \varepsilon_{yb} = -z\dfrac{\partial^2}{\partial y^2}(w - w_0) = \mathrm{z}\dfrac{\pi^2}{b^2}(W - W_0)\sin\dfrac{m\pi x}{a}\sin\dfrac{\pi y}{b} \\ \gamma_{xyb} = 2z\dfrac{\partial^2}{\partial x\partial y}(w - w_0) = 2\,\mathrm{z}\dfrac{m\pi^2}{ab}(W - W_0)\cos\dfrac{m\pi x}{a}\cos\dfrac{\pi y}{b} \end{cases} \tag{12}$$

In actual navigation, it is also necessary to consider the influence of environmental interference and model parameter uncertainty. Considering the existence of parameter uncertainty in ship models and external environmental interference, a neural network sliding mode adaptive control law is designed, which incorporates optimal vector information and has a faster convergence speed. However, it is also easy to fall into local optima as a result. To address this, a constraint function for ship obstacle-avoidance trajectory motion planning is constructed, and an improved particle swarm optimization algorithm is used to perform optimal parameter regression analysis and solve the ship obstacle-avoidance problem.

3. Optimization of ship obstacle avoidance trajectory motion

3.1 Particle Swarm Optimization Algorithm

The PSO algorithm using rotational surface transformation is used to monitor the current optimal function value of each particle. When it falls into a local minimum, collision avoidance is achieved through the artificial potential field method that jumps out of ship dynamic targets and static obstacles. This accurately describes the problem of collision avoidance path planning for unmanned watercraft on the water surface. This paper considers six practical requirements during navigation, including collision risk, turning amplitude, total range, collision avoidance rules, avoidance timing, and USV maneuverability [9]. The probability of particles taking 1 is higher, and vice versa is lower. The iterative algorithm is shown in the following equation:

$$x_{i,d}^{k+1} = \begin{cases} 1, & \rho_{i,d}^{k+1} \le sig\left(v_{i,d}^{k+1}\right) \\ 0, & \rho_{i,d}^{k+1} > sig\left(v_{i,d}^{k+1}\right) \end{cases} \tag{13}$$

In the above equation, $\rho_{i,d}^{k+1} \in [0,1]$ is a random number, $sig(\cdot)$ is a Sigmoid function, which is a velocity conversion function modeled as a multi-objective optimization problem. Among them, collision risk, total range, and turning amplitude play a dominant role, and their expressions are as follows:

ISSN 2616-5775 Vol. 9, Issue 8: 98-106, DOI: 10.25236/AJCIS.2026.090812

$$sig\left(v_{i,d}^{k+1}\right)=\frac{1}{1+e^{-v_{i,d}^{k+1}}} \tag{14}$$

For the sample set $\{(x_i, y_i)$, where x_i represents the input and y_i represents the corresponding output, the fitness function based on individual path points is:

$$f(x)=w^T\varphi(x)+b \tag{15}$$

In the formula, ω is the weight vector in collision avoidance decision-making, and b is the bias that has a significant impact on the avoidance effect.

Evaluating safety, steering range, and overall range economy through collision risk, and based on the principle of minimizing structural risk, the fitness of the entire path represents a constrained optimization problem:

$$\begin{aligned}&\min_{w,b,e} J(w,e)=\frac{1}{2}W^TW+\frac{C}{2}\sum_{i=1}^{n}e_i^2\\&s.t.\\&y_i=w^T\varphi(x)+b+e_i, i=1,2,\cdots,l\end{aligned} \tag{16}$$

In the formula, C is the penalty parameter; E_i is the prediction error of the trajectory.

By introducing Lagrange multipliers to decompose the objective function into individual path points, evaluate and optimize them separately, and establish a Lagrange function

$$L(w,b,e,\alpha)=J(w,e)-\sum_{i=1}^{l}\alpha_i\left(w^T\varphi(x_i)+b+e_i-y_i\right) \tag{17}$$

In the equation, α_i is the Lagrange multiplier. By decomposing the entire path into path points based on their positions or geometric relationships, combined with KKT conditions, we can obtain

$$\begin{bmatrix}0 & e1^T\\ e1 & Q+C^{-1}I\end{bmatrix}\begin{bmatrix}b\\ a\end{bmatrix}=\begin{bmatrix}0\\ y\end{bmatrix} \tag{18}$$

Among these,

$$\begin{cases}y=(y_1,y_2,\cdots,y_l)^T\\ e1=(1,1,\cdots,1)^T\\ a=(a_1,a_2,\cdots,a_l)^T\end{cases} \tag{19}$$

In the formula, I represents the identity matrix, $Q_{ij}=\left(\varphi(x_i)\varphi(x_j)\right)$. For the planned USV navigation path, the total range is an economic evaluation indicator, which is decomposed according to the path points. That is, the calculation of the minimum distance of the entire path is transformed into the calculation of the distance between two adjacent path points on the path. The LSSVM classification decision function for particle swarm optimization is obtained as follows:

$$f(x)=\mathrm{sgn}\left(\sum_{i=1}^{n}\alpha_iF(x,x_i)+b\right) \tag{20}$$

In the equation, σ is the width parameter of the radial basis kernel function. In each path, optimization is performed in ascending order of path points, and the information of the i-th path point in the population can be used to improve the quality of the currently evolving path point.

ISSN 2616-5775 Vol. 9, Issue 8: 98-106, DOI: 10.25236/AJCIS.2026.090812

3.2. Implementation of obstacle avoidance planning

The improvement principle of the objective function based on the total distance is similar. Taking the second to last path point in the current path as the i-th path point, the (i+1) th path point is taken as the destination. Taking the point where x=0 and y=0 as an example, due to the non loaded edge simple support, the information of the i-th path point in the population is used to improve the currently evolving path, which can be expressed as:

$$\sigma_{\text{eq1}} = \sqrt{\sigma_{xp}{}^2 + \sigma_{yp}{}^2 - \sigma_{xp}\sigma_{yp}} \tag{21}$$

In the process of collision path planning, the first condition that should be met is safe and effective avoidance. Collision avoidance and obstacle avoidance actions should follow the principles of "early", "large", "wide", and "clear" to minimize the collision risk of the entire route [10]. The distance between the target ship or obstacle can be expressed as:

$$\sigma_{\text{eq2}} = \sqrt{\sigma_{xp}{}^2 + \sigma_{yp}{}^2 - \sigma_{xp}\sigma_{yp}} \tag{22}$$

When the maximum value of collision risk is the smallest compared to the maximum values of other schemes, this scheme is the safest. The objective function based on collision risk can be expressed as:

$$\sigma_{\text{eq3}} = \sqrt{(\sigma_{xp} + \sigma_{xb})^2 + (\sigma_{yp} + \sigma_{yb})^2 - (\sigma_{xp} + \sigma_{xb})(\sigma_{yp} + \sigma_{yb})} \tag{23}$$

By comparison, it can be concluded that $\sigma_{\text{eq1}} \le \sigma_{\text{eq2}}$ and $\sigma_{\text{eq1}} \le \sigma_{\text{eq3}}$, the yielding ship should immediately give way. Set the objective function based on avoidance timing as follows:

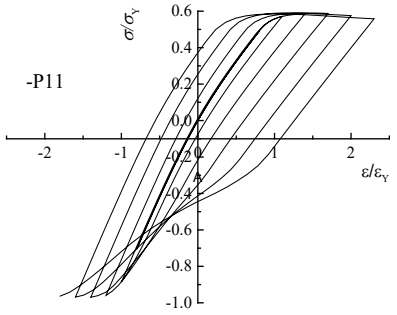
$$S = a_{11}K_{\text{I}}^2 + 2a_{12}K_{\text{I}}K_{\text{II}} + a_{22}K_{\text{II}}^2 + a_{33}K_{\text{III}}^2 \tag{24}$$

Appropriate avoidance timing can ensure that unmanned surface vessels take collision avoidance measures at the appropriate time, which not only avoids the decrease in navigation efficiency caused by excessive avoidance in advance, but also prevents collision risks caused by slow response. Monitoring the current optimal function value of each particle, when it falls into a local minimum, collision avoidance is achieved through the artificial potential field method of jumping out of ship dynamic targets and static obstacles. The introduction of target point position factor improves the gravitational potential field function, achieving high-precision planning and design of ship obstacle avoidance trajectory motion.

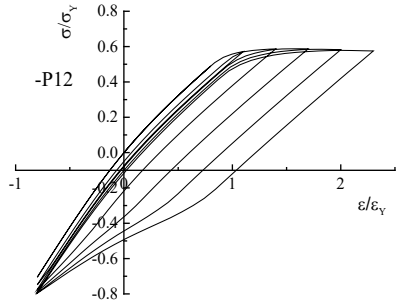
4. Simulation experiment

The simulation experiment environment is set in open water with good visibility, without considering external interference such as wind, waves, and currents. Following the usual practices of COLREGs and sea vessel crew, when the vessel is making way for other vessels, it adopts a turning method to avoid them. Three simulation encounter scenarios were constructed based on the above conditions. In the comparative experiment, the common parameters of particle swarm optimization algorithm, genetic algorithm, A * algorithm, and improved differential particle swarm optimization algorithm were set as follows: iteration number M=100, population size NP=50, population dimension Q=10, ω_1=0.4, ω_2 =0.1, ω_3 =0.5. The segmented avoidance process diagram of the paths planned by the four algorithms is shown in Figure 1.

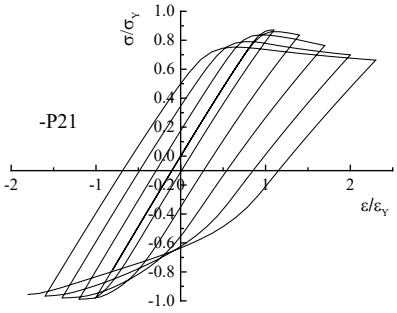
ISSN 2616-5775 Vol. 9, Issue 8: 98-106, DOI: 10.25236/AJCIS.2026.090812



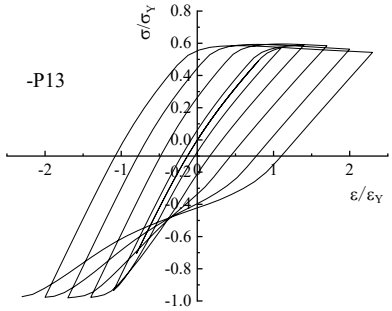
(a)PSO



(b) Genetic Algorithm



(c)A algorithm*



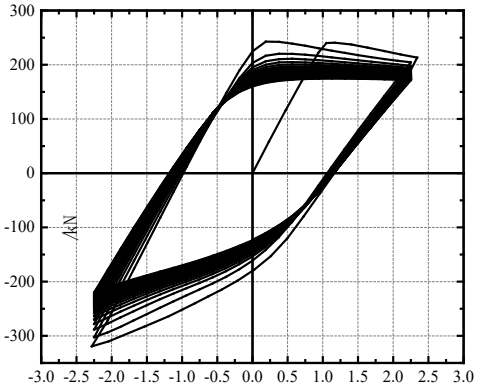
(d) Improved differential particle swarm optimization algorithm

Figure 1 Segmented avoidance process of paths planned by four algorithms

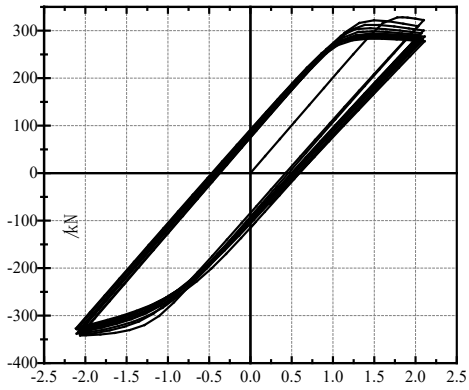
Comparing the collision avoidance paths of four algorithms, both A * algorithm and genetic algorithm avoided static obstacles at a safe distance. However, in the case of vertical intersection, they did not follow the COLREGs to turn right for avoidance. During the process of turning left, they were too close to the target ship, which increased the risk of collision. In addition, the genetic algorithm deviated from the original route for a long time, resulting in poor economy. The particle swarm optimization algorithm and the improved differential evolution algorithm follow the COLREGs and adopt the avoidance strategy of turning to the right and passing through the stern of the target ship. However, compared with the two, the particle swarm optimization algorithm avoids collision later and only starts turning when it is relatively close to the target ship, without sufficient avoidance. After clearing, it leads to a path slightly closer to static obstacles, and the overall safety is not as good as the improved differential evolution algorithm. Moreover, the maximum yaw distance is slightly larger than that of the improved differential planning algorithm; The improved differential evolution algorithm not only follows collision avoidance rules, but also meets the requirements of "early", "large", "wide", and

ISSN 2616-5775 Vol. 9, Issue 8: 98-106, DOI: 10.25236/AJCIS.2026.090812

"clear". The closest distance to dynamic ships is 0.94 nautical miles, and the closest distance to obstacles is 1.13 nautical miles. The segmented avoidance process diagram of the paths planned by the four algorithms is shown in Figure 2.



(a) Genetic Algorithm



(b) Improved particle swarm optimization algorithm

Figure 2 shows the segmented avoidance process of the planned path

Comparing the collision and obstacle avoidance paths of two algorithms, the A * algorithm plans a path that passes through the area between target ship 1 and target ship 2, requiring simultaneous avoidance of two dynamic ships. During the avoidance process, the distance to both target ships is relatively close, which poses a high risk and improves the efficiency of data. The accuracy of ship collision avoidance before improvement has increased from 82.5% to 92.5%. Among them, particle swarm optimization algorithm can return to the original planned route and travel towards the destination, while genetic algorithm has a significant deviation after avoidance. Improved particle swarm evolution algorithm can ensure safe avoidance of target ships and static obstacles, with a smaller distance deviation from the original planned route, which meets the requirements of practical operation and is more economical.

5. Conclusions

In this article, a high-precision simulation model of ship obstacle avoidance trajectory motion based on improved particle swarm optimization algorithm is proposed. The parameter model and kinematic model of ship obstacle avoidance trajectory motion are constructed, and the PSO algorithm with rotating surface transformation is used to monitor the current optimal function value of each particle. When it falls into the local minimum value, collision avoidance is carried out through the artificial potential field method that jumps out of the ship's dynamic targets and static obstacles. The fitness value of this method is lower, the planned path quality and smoothness are higher, and the safe distance between the ship and the target in different scenarios is not less than 0.82 nautical miles, which can fully reflect the adaptability to COLREGs. The total range is shorter, the economy is better, and it can return in a timely manner. This verifies the effectiveness of this method in multi-target encounter scenarios. The effectiveness of strategies for collision avoidance and obstacle avoidance was evaluated.

ISSN 2616-5775 Vol. 9, Issue 8: 98-106, DOI: 10.25236/AJCIS.2026.090812

References

[1] WANG Yufang, PEI Xiaohong, YAN Ming. Multi-Strategy Improved Water Wave Optimization Algorithm and Its Application[J]. Computer Engineering and Applications, 2025, 61(18): 99-113.
[2] CHENG Y L, LI S Q. Snake optimization algorithm based on chaotic reverse and Levy flight[J]. Computer Engineering and Design, 2024, 45(9): 2658-2668.
[3] LI J H, WANG P H, LI W. A hybrid multi-strategy improved sparrow search algorithm[J]. Computer Engineering & Science, 2024, 46(2): 303-315.
[4] CHEN L F, CAO K X, ZHANG S P, et al. Recent progress of swarm intelligent optimization algorithms[J]. Computer Engineering and Applications, 2024, 60(19): 46-67.
[5] YANG Zhiyuan, LUO Liang, WU Tianyang, YU Boxiang. Improved Lightweight Ship Target Detection Algorithm for Optical Remote Sensing Images with YOLOv8[J]. Computer Engineering and Applications, 2024, 60(16): 248-257.
[6] Wang Zhen, Sang Hongqiang, Sun Xiujun. Obstacle Avoidance Method of Wave Glider Formation[J]. Science Technology and Engineering,2022,22(21):9176-9181.
[7] XIONG Yong, ZHANG Jia, YU Jiajun, ZHANG Benren, LIANG Xuanzhuo, ZHU Qige. Intelligent layout optimization algorithm for 3D pipelines of ships[J]. Journal of Computer Applications, 2020, 40(7): 2164-2170.
[8] Lingxia MU, Zhengjun ZHOU, Ban WANG, Youmin ZHANG, Xianghong XUE, Kaikai NING. Formation obstacle-avoidance and reconfiguration method for multiple UAVs[J]. Journal of Computer Applications, 2024, 44(9): 2938-2946.
[9] LI Minggui, ZHOU Huanyin, GONG Liwen. Comprehensive Review of ROV Underwater Obstacle Detection and Avoidance Technology[J]. Computer Engineering and Applications, 2024, 60(17): 34-47.
[10] CAO X, REN L, SUN C. Research on obstacle detection and avoidance of autonomous underwater vehicle based on forward-looking sonar[J]. IEEE Transactions on Neural Networks and Learning Systems, 2023, 34(11): 9198-9208.